RSC Advances

PAPER

View Article Online
View Journal | View Issue

Cite this: *RSC Adv.*, 2020, **10**, 43629

Formulation development, *in vitro* and *in vivo* evaluation of chitosan engineered nanoparticles for ocular delivery of insulin

Priyanka Rathore,[a] Alok Mahor,*[b] Surendra Jain,[a] Anzarul Haque[c] and Prashant Kesharwani *[d]

Insulin-dependent diabetic patients have to count on the administration of painful and discomforting insulin injections. However, inadequate insulin absorption and the risk of insulin level escalation in the blood are some disadvantages associated with insulin therapy. Thus, the current study intends to formulate insulin-loaded chitosan nanoparticles for refining the systemic absorption of insulin *via* the ocular route. Insulin-loaded chitosan nanoparticles were prepared by the ionotropic gelation method and characterized for various parameters. Optimized insulin loaded nanoparticles (C4T4I4) were positively charged with a particle size of 215 ± 2.5 nm and showed 65.89 ± 4.3% entrapment efficiency. The *in vitro* drug release exhibited sustained release of insulin, where 77.2 ± 2.1% of release was observed after 12 h and leads to an assumption of the non-Fickian diffusion release mechanism. The permeation study discloses good mucoadhesive and better permeation properties of insulin loaded nanoparticles compared to free Insulin. No significant difference was observed in the size of particles after six months of storage, signifying their adequate stability. Nanoparticles were found to be non-irritant to ocular tissues and exhibited prominent blood glucose level reduction *in vivo*. The outcomes of this study suggested that the chitosan nanoparticulate system could act as a prominent carrier system for insulin with enhanced stability and efficacy.

Received 6th September 2020
Accepted 8th November 2020

DOI: 10.1039/d0ra07640f

rsc.li/rsc-advances

1. Introduction

Peptides and protein drugs like insulin for diabetes management are compelling therapeutic agents. Due to high molecular weight, lack of defence against enzymatic degradation,[1] and inability to cross intestinal mucosa,[2] it is always challenging to administer proteins and peptides such as insulin, orally. Though subcutaneous injections are effective in regulating blood glucose levels, parenteral administration of insulin necessitates recurring injections because of their enormously short biological half-life and has been an area of concern relating to patient acquiescence.

Thus, it turned out to be obligatory to reconnoiter various non-invasive routes for insulin delivery such as pulmonary,[3] colonic,[4] nasal,[5] buccal,[6] transdermal,[7] intraperitoneal,[8] rectal.[1] However effective, the aforementioned routes displayed low insulin bioavailability when equated to subcutaneous injection. Nevertheless, the ocular route has offered a hopeful way for the systemic delivery of insulin.[9] Although, a few trepidations in ocular delivery of drugs exist, *e.g.* deprived transport across epithelia, which leads to poor bioavailability due to drug loss. Thus, the efficacy of a topically administered drug delivery system depends on interaction with the ocular mucosa, protection from degradation, and facilitation of delivery to the ocular tissues.[10]

Several reports have been published describing the delivery of drugs *via* the ocular route. Poly(alkylcyanoacrylate) (PACA) nanoparticles[11] and poly-ε-caprolactone nanocapsules[12] efficaciously augmented the intraocular penetration of drugs. These nanoparticles were able to interact and transport across the corneal epithelium.[13] This transport could be well attributed to the colloidal nature of the nanoparticles[14] though, short residence time at the ocular surface was the major constraint of these nanoparticles. Therefore, the use of mucoadhesive polymers possibly could curtail this limitation.[15]

Chitosan has been explored as a material of choice to form nanoparticle for the last few decades.[16] Being a biocompatible, mucoadhesive, and cationic polymer, it augments the perviousness of the biological membrane and eases the mucoadhesion by ionic interaction of positive CS amino groups with the negatively charged sialic acid residues in mucous at the corneal surface.[17]

[a]*Sagar Institute of Research and Technology Pharmacy, Bhopal, India*

[b]*Institute of Pharmacy, Bundelkhand University, Jhansi, India. E-mail: dralokmahor@gmail.com; Tel: +91 9889395119*

[c]*Department of Pharmacognosy, College of Pharmacy, Prince Sattam bin Abdul Aziz University, Alkharj, Kingdom of Saudi Arabia*

[d]*Department of Pharmaceutics, School of Pharmaceutical Education and Research, Jamia Hamdard, New Delhi, 110062, India. E-mail: prashantdops@gmail.com; Fax: +91-7999710141; Tel: +91-7999710141*

Gupta *et al.*, 2010[18] developed a chitosan and gellan gum-based novel *in situ* gel system loaded with timolol maleate which showed enhanced ocular retention time and was non-irritant and tolerable to ocular tissues. Apart from boosting the delivery of the entrapped drug molecule, chitosan offers fortification to the encapsulated drug as well as increases its clearance time and stability in the body. Several studies have been published discussing the utility of chitosan nanoparticles for the delivery of insulin *via* ocular, vaginal, rectal, and oral (buccal, gastro-intestinal) routes.[19,20] Tripolyphosphate has been used as a crosslinking agent in the fabrication of chitosan nanoparticles as TPP has a high negative charge density to interact with polycationic chitosan. Crosslinking of TPP with chitosan at a certain ratio aids in the formation of nanoparticles and provides mechanical strength to the nanoparticles formed and renders them strong enough to split into smaller particles.[21]

The eye is protected by a layer of sclera and cornea and isolated by a blood ocular barrier. Moreover, the cornea is structurally unique and contradictory to any biological membrane, in which an aqueous phase (stroma) layer is present in between two layers of lipid (epithelium and endothelium). This unique structure allows two types of delivery through the eye: (a) delivery through the cornea and (b) delivery *via* the nasolacrimal system, through which the drug will reach systemic circulation without entering inside the eye system.[22]

The ocular route is an open window for delivering protein and peptides using adjuvants or permeation enhancers. However, ocular delivery of such agents like insulin is challenging mainly because of the large size, hydrophilicity, and instability of these macromolecules.

Thus, the entrapment of insulin within the nanoparticulate carrier system could be a good approach to upsurge the bioavailability of insulin *via* ocular administration. Effective systemic absorption of insulin loaded in nanoparticles *via* the ocular route has been reported on several occasions.[23] Srinivasan and Jain, 1998, efficaciously delivered insulin loaded liposomes *via* the ocular route for the management of blood glucose levels.[24] Yamamoto *et al.*, 1989 (ref. 25) reported that bioavailability of insulin in rabbits was less than 1% when administered topically *via* ocular route due to minimal systemic absorption of the drug as the absorption is largely constrained by substantial lacrimal drainage.

Following the above findings and cautiously probing the inadequacies of insulin delivery *via* other routes, here in this study, insulin loaded chitosan nanoparticles were designed and assessed for systemic absorption of insulin *via* the ocular route. The novelty of this research lies in the formulation itself as it proposes the use of a biodegradable polymer excluding the use of harsh chemicals. The ratio of the polymer/crosslinker would ensure the preparation of optimum sized nanoparticles, and the positively charged chitosan will provide adherence to the negatively charged ocular surface.

Also, the optimized formulation will protect the encapsulated insulin from the first-pass metabolism. Physicochemical characterization and pharmacological performance of the developed nanoparticles has been carried out to assess ocular residence and permeation. To the best of our knowledge, few works of literature are available showing the potential of chitosan nanoparticles for ocular delivery of insulin.

2. Materials and methods

2.1. Materials

Insulin was procured as a gift sample from Torrent Pharmaceuticals Ltd. Ahmedabad, India. Chitosan was obtained as a gift sample from the Central Institute of Fisheries, Kochi, India. Tripolyphosphate, sodium hydroxide, sodium chloride, disodium hydrogen phosphate, potassium dihydrogen phosphate, and dialysis membrane (molecular weight cut off 12 000–14 000 Dalton) were purchased from Himedia, India. All other chemicals used were purchased from Sigma Aldrich (St. Louis, MO) and were of the highest analytical reagent (AR) grade.

2.2. Animals

The *in vivo* studies were performed on male New Zealand albino rabbits (1.5–2.0 kg), devoid of any oddity of ocular inflammation and uncultured malformations. Animals were familiarized with the customary laboratory conditions in a cross aerated animal housing at a temperature of 25 ± 2 °C and 75% relative humidity with light and dark cycles of 12 : 12 h. They were fed a laboratory diet and water *ad libitum* throughout the studies. All the animal experiments were granted permission by the Institutional Animal Ethical Committee of the Patel College of Pharmacy, Madhyanchal Professional University, Bhopal, India, with the approval number: EP/PEP/19/C1309 and have been conducted in accordance with the standard and guidelines laid down by the Committee for the Purpose of Control and Supervision of Experiments on Animals (CPCSEA), Ministry of Social Justice and Empowerment, Government of India.

2.3. Preparation of nanoparticles

Chitosan nanoparticles were prepared by ionotropic gelation of chitosan with tripolyphosphate (TPP) anions as reported by Calvo *et al.*[26] Chitosan solution was prepared by dissolving 100 mg of chitosan (1% w/v) in acetate buffer with the aid of sonication. Insulin was then added to the chitosan solution followed by a dropwise addition of 2 ml of TPP solution (in water) to the 3 ml of the above mixture. The nanoparticles were formed spontaneously upon the incorporation of a variable volume of TPP solution (Table 1) into chitosan solution, under magnetic stirring at room temperature. Ionotropic gelation occurs when the positively charged amino group of chitosan interacts with negatively charged TPP, through inter and intra linkages created between TPP phosphates and chitosan amino groups.

The final dispersion of nanoparticles (pH 5.6) was concentrated by centrifugation at 10 000 rpm for 30 min and the sediment was washed with water. Supernatants were collected for the measurement of the entrapment efficiency and the sediment (nanoparticles) were re-suspended in phosphate buffer (pH 7.4). Blank particles were prepared similarly without using insulin for comparison purposes.

Table 1 Formulation, % entrapment efficiency, particle size, and zeta potential of the insulin loaded chitosan nanoparticles[a]

Formulation	CS : TPP : INS	%EE	Size (nm)	PDI	€ (mv)
C1T1I1	1 : 0.1 : 1	44.25 ± 3.4	282 ± 3.0	0.41 ± 0.02	+30.6 ± 1.5
C2T2I2	1 : 0.2 : 1	53.56 ± 5.1	273 ± 1.3	0.57 ± 0.07	+27.3 ± 2.5
C3T3I3	1 : 0.3 : 1	60.62 ± 6.3	255 ± 2.3	0.34 ± 0.09	+24.1 ± 1.8
C4T4I4	1 : 0.4 : 1	65.89 ± 4.3	215 ± 2.5	0.27 ± 0.08	+22.8 ± 1.2
C5T5I5	1 : 0.5 : 1	61.21 ± 4.5	240 ± 1.5	0.21 ± 0.08	+20.6 ± 1.1
C6T6I6	1 : 0.6 : 1	59.02 ± 3.1	249 ± 6.8	0.23 ± 0.09	+17.6 ± 2.1

[a] All values are presented as mean ± SD, $n = 3$.

2.4. Characterization of nanoparticles

2.4.1. Particle size distribution and morphology. The mean particle size and size distribution (PDI) of nanoparticles were determined by photon correlation spectroscopy (PCS). Samples were diluted to 50 μg ml^{-1} with purified water. The surface charge of insulin loaded chitosan nanoparticles (diluted in deionized water before zeta potential measurement) was calculated from mean electrophoretic mobility values which were determined by Laser Doppler Anemometry (LDA). The PCS and LDA analysis were performed using a zeta-sizer, NanoZS (Malvern Instruments, UK).

The surface morphology of particles was determined using Scanning Electron Microscopy (SEM) (LEO 435 VP, Eindhoven, Netherland) at 5.0 kV. The samples were prepared by scattering the lyophilized chitosan nanoparticles on an aluminum stub layered with gold with a thickness of about 300 Å.

2.4.2. Percentage entrapment efficiency.[27] The % entrapment efficiency of insulin loaded chitosan nanoparticles was determined by sonicating the accurately weighed freeze-dried optimized nanoparticles (10 mg). The sample was dissolved in 2 ml of 0.1 N HCl and was sonicated for 5 minutes to dissolve the insulin. 1 ml of the collected sample was further diluted with PBS (pH 7.4) up to 5 ml and was centrifuged at 5000 rpm for 5 minutes. The collected supernatant containing free insulin was analyzed *via* HPLC (Shimadzu, Japan) armed with a quaternary pump. The mobile phase consisted of phosphate buffer (pH 2.5) and acetonitrile and was run isocratically at a flow rate of 1 ml min^{-1}. The UV detector was set at λ_{max} of 270 nm with a reversed-phase X-Terra RP 18 column 5 μm, (Merck, Germany). The injection volume was set at 100 μl. The % entrapment efficiency can be determined using the following formula:[28]

$$\%\text{Entrapment efficiency} = \frac{\text{CSN}_{(\text{Act})}}{\text{CSN}_{(\text{Theo})}} \times 100 \quad (1)$$

where $\text{CSN}_{(\text{Act})}$ is the actual amount of drug in the weighed quantity of nanoparticles and $\text{CSN}_{(\text{Theo})}$ is the theoretical amount of drug in the nanoparticles calculated from the quantity added in the process.

2.4.3. Physicochemical characterization

2.4.3.1. FTIR spectroscopy. Fourier transform infrared spectroscopy (FTIR) of insulin, chitosan, insulin loaded nanoparticles as well as unloaded nanoparticles were obtained by preparing KBR pellet of the samples and analyzing them using FTIR spectrometer (Shimadzu-1800, Japan). The % Transmittance (% T) was recorded in the spectral region of 4000–500 cm^{-1}.

2.4.3.2. Differential scanning calorimetry. Thermal activities of insulin, blank chitosan particles, and the insulin loaded chitosan nanoparticles were obtained through DSC-60 cell (Shimadzu, Japan) using aluminum crucibles with about 2 mg of the sample under nitrogen gas stream. Investigations were carried out over the temperature range of 30–400 °C with a heating flow rate of 10 °C min^{-1}.

2.5. *In vitro* studies

2.5.1. *In vitro* drug release studies. To assess the insulin release from nanoparticles, 455 μg of optimized insulin loaded chitosan nanoparticles (contains 10 IU ml^{-1} insulin) were suspended in 1 ml of simulated artificial tear fluid (SATF, pH 7.2) and were sealed in a dialysis bag (m.wt.12 kDa, Sigma Aldrich, USA). The bag was kept immersed in 25 ml of SATF at 37 ± 2 °C under magnetic stirring. Samples were withdrawn at predetermined intervals and were replaced by the same volume of fresh simulated tear solution to hold sink condition during the whole experiment. Samples were analyzed by reverse-phase HPLC method.[29] All experiments were done in triplicate and ±SD was calculated.

2.5.2. *Ex vivo* transcorneal permeation studies. From a local slaughterhouse, Bhopal, India, the goat corneas were excised and collected immediately after the animal sacrifice and were placed in an ice-cold (4 °C) Kreb's buffer in which oxygen was continuously bubbled. Each cornea was placed between the donor and the acceptor chamber of Franz diffusion cells and oxygen was bubbled into simulated tear buffer (pH 7.4) present in both chambers. To quantify the transport of the optimized formulation through the cornea, the buffer of the donor chamber was replaced by 1 ml of formulation (Insulin NPs – 10 IU ml^{-1} or 455 μg ml^{-1}).

In another setup, the buffer of the donor chamber was replaced by an insulin solution with a similar concentration for comparison purposes. To study the corneal permeation of the nanoparticles, the perfusate was collected at periodic time interval *i.e.* 1, 3, 6, and 12 h from the acceptor chamber and centrifuged at 10 000 rpm for 30 minutes; the supernatant was collected and analyzed by HPLC (Shimadzu, Japan) to determine the insulin concentration.[30]

2.6. *In vivo* studies

The *in vivo* studies were performed on male New Zealand albino rabbits (1.5–2.0 kg), devoid of any oddity of ocular inflammation and uncultured malformations. Animals were familiarized with

the customary laboratory conditions in a cross aerated animal housing at a temperature of 25 ± 2 °C and 75% relative humidity with light and dark cycles of 12 : 12 h. They were fed laboratory diet and water ad libitum throughout the studies. All the animal experiments were granted permission by the Institutional Animal Ethical Committee of the Patel College of Pharmacy, Madhyanchal Professional University, Bhopal, India, with the approval number: EP/PEP/19/C1309 and have been conducted in accordance with the standard and guidelines laid down by the Committee for the Purpose of Control and Supervision of Experiments on Animals (CPCSEA).

2.6.1. *In vivo* tolerance studies. To assess the biocompatibility and safety of the nanoparticles at the corneal surface, an ocular irritation test was performed.[31] For this study, a single instillation of 50 μl of optimized formulation C4T4I4, plain insulin, and control (simulated artificial tear fluid {SATF, pH 7.4}) was administered to nine New Zealand albino rabbits (three groups, comprising of three animals in each group) respectively in the morning at the animal house.

The test was performed employing a clinical evaluation scale of zero (absence) to three(highest) and animals were observed for alteration in normal discharge, discomfort, alteration in normal morphology of cornea, conjunctiva, eyelids. Each animal was observed at 0.5, 2, 4, and 16 h after instillation. An index of overall irritation was calculated by summing up the total clinical evaluation scores over the observation time.

2.6.2. *In vivo* anti-diabetic studies. Nine rabbits were used to assess the antidiabetic potential of the insulin loaded chitosan nanoparticles. Three groups were assigned with three animals in each group. All animals (15 in total for induction of diabetes) were given an intravenous injection of streptozotocin solution in citrate buffer pH 5.0 (65 mg kg^{-1}) for three days for the induction of diabetes in the evening. On the fourth day morning, animals that showed fasting blood glucose level more than 300 mg dL^{-1} confirmed initiation of diabetes were reserved for study antidiabetic studies (9 in total out of 15).

Blood glucose level was estimated on day 1 after overnight fasting *i.e.* normal glucose level. Animals of group I received blank nanoparticles (control) whereas animals of II and III group received insulin loaded nanoparticles (10 IU Kg^{-1}) and plain insulin (10 IU Kg^{-1}) respectively into either eye with the help of the calibrated eye dropper. Blood samples were withdrawn carefully by capillary from the retro-orbital sinus into the centrifuged tubes. Blood glucose level was estimated using GOD/POD glucose estimation kit in the autoanalyzer Rh 50, and before the estimation autoanalyzer was calibrated using standards.[32,33] The % reduction in blood glucose level was assessed using the formula;

$$\%\ \text{Reduction in blood glucose level} = \frac{\text{Blood glucose level [before drug administration} - \text{after drug administration]}}{\text{[Blood glucose level before drug administration]}} \times 100 \quad (2)$$

2.6.3. Pharmacokinetic studies. Nine New Zealand albino rabbits (1.5–2.0 kg body weight, divided into three animals into four groups), were utilized to assess the pharmacokinetic performance of the developed chitosan nanoparticles. The plasma insulin levels of insulin loaded chitosan particles were compared with the plain insulin solution (5 IU kg^{-1}, *via* the ocular route) and with the subcutaneous human insulin solution (5 IU kg^{-1}). All animals were fasted before and during the progression of the experiment but were permitted to access water *ad libitum*.

The I^{st} group received a subcutaneous injection of human insulin solution (5 IU kg^{-1}). To the II^{nd} group, C4T4I4 (5 IU kg^{-1}) was instilled into the eye and the III^{rd} group was instilled with plain insulin solution (5 IU kg^{-1}) ($n = 3$). Blood samples were collected *via* ear pinna of the test animals, centrifuged for 15 minutes at 10 000 rpm, at 4 °C, and plasma insulin levels were quantified using HPLC (Shimadzu, Japan).

Various pharmacokinetic parameters such as maximum drug concentration (C_{max}) and the time of maximum drug concentration (T_{max}) were escalated from concentration *vs.* time profiles.[34] Employing the trapezoidal method, the area under the concentration–time curve (AUC_{0-12}) was estimated. To evaluate the statistical difference between the treatments for the extent of drug absorption in both ocular tissues (AUC_{0-12}), a paired *t*-test (at $P < 0.01$) was used.[35] Data are presented as mean ± SD. A variation of $P < 0.05$ was considered statistically significant.

2.7. Stability studies

Stability studies were conducted following WHO guidelines on optimized batch C4T4I4. The sample batches were stored at 4 ± 1 °C and 25 ± 1 °C. Upon six months of storage, all samples were analyzed for particle size, and % drug entrapment efficiency, and the results were compared with the initial values.

2.8. Statistical analysis

In this study, all data are represented as mean ± standard deviation ($n = 3$). Statistical analysis was conducted using multiple *t*-test and a significant difference ($P < 0.05$) was determined using the Holm–Sidak method, with alpha = 5.000%. All statistical analysis was performed on graph-pad Prism software (version-6.01).

3. Results and discussion

3.1. Nanoparticle preparation and characterization

Chitosan nanoparticles were prepared *via* vastly explored ionic gelation method. For optimization purposes, the TPP ratio was changed to assess the effect on entrapment efficiency and size (Table 1). Earlier studies suggested that the insulin loading within chitosan particles was mediated by electrostatic interaction between positively charged chitosan and negatively

charged insulin. Insulin activity and its hypoglycaemic effect did not change upon the electrostatic interaction with chitosan as indicated in the results obtained in *in vivo studies.*[36]

It was observed that the TPP ratio used in the range of 0.1 to 0.4 influenced the particle size, zeta potential, and percent drug entrapment efficiency of the prepared nanoparticles. Amongst all the batches, C4T4I4 yielded the least particle size with the highest drug entrapment efficiency (Table 1). The particle size decreased on increasing the concentration of TPP but after a certain ratio, an increment in TPP concentration leads to an increase in particle size. This could be accredited to the less uniform ionic interaction between chitosan and TPP at a lower ratio, but at a certain ratio in this study, the optimum linkage between CS and TPP was observed, resulting in a smaller size of particles (Fig. 1a). However, on further increment in TPP concentration, particle size increases due to the saturation of the interaction site on chitosan which results in adherence of excess TPP anions on positively charged surfaces of chitosan.[37]

Zeta potential declined as the TPP concentration is increased, which could be ascribed to the presence of a lesser number of unbound positively charged sites of chitosan, as both TPP and insulin excite for binding to free positive amino sites of chitosan[38] (Fig. 1b). The high zeta potential on the nanoparticles suggested good stability of the formulation because of electrostatic repulsion between the positively charged chitosan nanoparticles preventing aggregation and strong electrostatic contact with the negatively charged sialic acid residues of mucin in the ocular surface.[39,40] Lower PDI values were observed (indicating the formation of a homogenous dispersion) for the formulations as the TPP ratio was increased (Table 1).

SEM photographs of nanoparticles (Fig. 2a) show nearly spherical particles with close to smooth surfaces. Larger particles as seen in Fig. 2b may be due to the accretion of smaller particles into a bulky unit.

3.2. Percentage entrapment efficiency (%EE)

The batch C4T4I4 demonstrated the highest entrapment efficiency in comparison to other batches (Table 1). The effect of TPP concentration on drug entrapment efficiency was studied, and it was found that on increasing the concentration of TPP up to a certain ratio, the entrapment efficiency of nanoparticles increased. This could be attributed to the reduction in size and results in an increased surface area of the nanoparticulate matrix, which results in the availability of more space for drug encapsulation. As we increased the TPP ratio (above 0.4), the % entrapment efficiency decreased due to the contending interaction between TPP and insulin for chitosan binding.

Thus, it can be concluded that the optimum ratio of chitosan and TPP (1 : 0.4) led to the formation of uniform shape and size nanoparticles with the highest %EE. However, drug incorporation seems to be related not only to electrostatic interaction but also to physical process and/or absorption phenomena. The validation method of insulin by HPLC produced a linear response over the concentration range of 10–100 μg ml^{-1} with a mean recovery of 97 ± 0.20% as well as average intra and inter-day variations of 1.45 and 4.52% respectively. The limits of detection (LOD) and quantitation (LOQ) were 0.32 and 0.68 μg ml^{-1} respectively.

3.3. Physicochemical characterization

To confirm CS/TPP interaction as well as insulin entrapment into chitosan nanoparticles, chitosan powder, insulin, drug-loaded, and unloaded nanoparticles were analyzed by FTIR

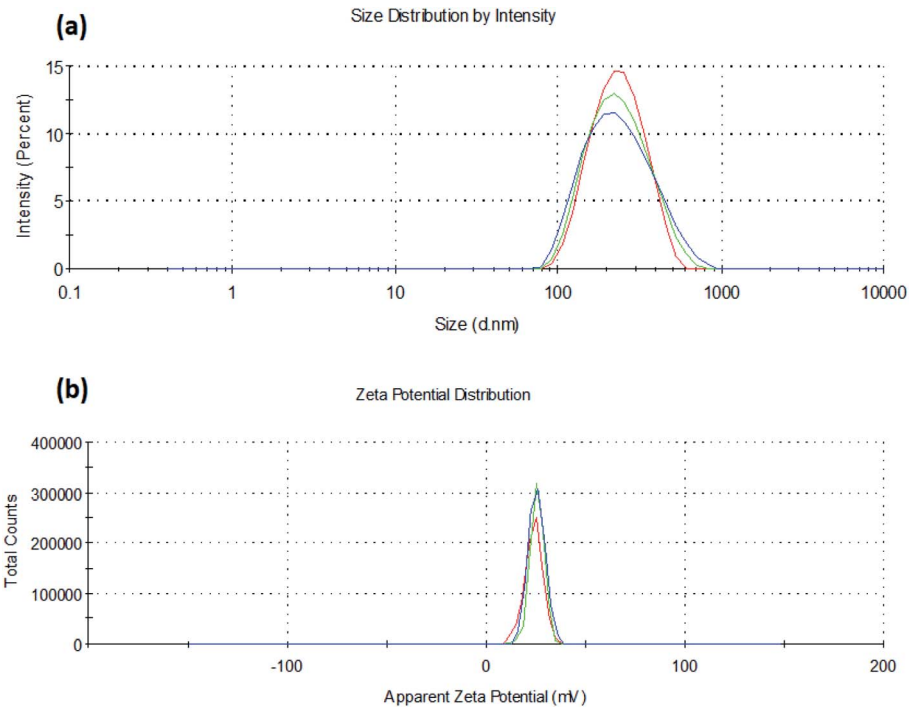

Fig. 1 (a) Particle size and (b) zeta potential of insulin loaded chitosan nanoparticles (C4T4I4).

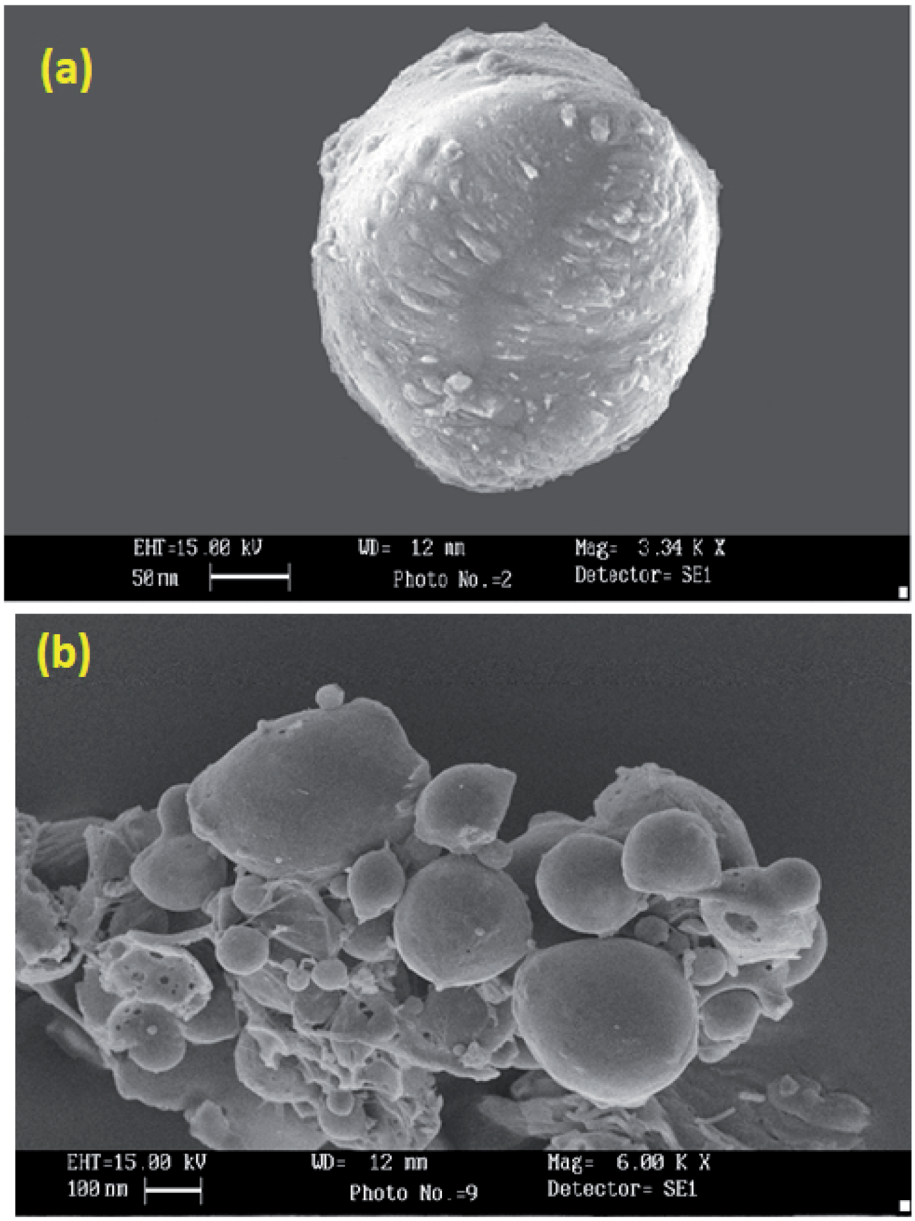

Fig. 2 Scanning electron micrograph of C4T4I4 (a) and C4T4I4 (cluster) (b).

spectroscopy. Fig. 3a depicts the FTIR spectra of chitosan, insulin, placebo, and insulin loaded nanoparticles. Spectra of chitosan reveal that a band at 3424 cm^{-1} has been attributed to –OH group stretching vibration in chitosan matrix, a peak at 1660 cm^{-1} of chitosan amine was observed and a peak around 1250 cm^{-1} was also observed for ether available on chitosan structure.[41] Insulin showed a characteristic peak in the region of 3310, 1650, and 628 cm^{-1}. In unloaded chitosan nanoparticles, the peak of chitosan amine at 1660 cm^{-1} was shifted to 1645 cm^{-1} and the formation of a new peak at 1565 cm^{-1} indicated bond formation between the amino group of the polymer chain and the phosphate group of TPP anion. The peaks of chitosan and insulin were transformed in the insulin loaded chitosan nanoparticles as the intensity of these peaks were lowered in insulin loaded chitosan nanoparticles. The insulin spectrum exposed two peaks on the nanoparticle's absorption bands at the amide I (~1647 cm^{-1}) and amide II (~1541 cm^{-1}) mainly due to C=O stretching vibration, which is characteristic of protein structure.[42] Peak intensity was significantly reduced which could be well attributed to weak insulin–chitosan interaction signifying entrapment of insulin into the nanoparticles.

The differential scanning thermogram of chitosan exhibited a low endothermic peak at 54 °C indicating loss of water molecules.[43] Thermal decomposition of chitosan was observed with a broad peak around 330 °C. DSC curve of pure insulin displayed low-intensity peaks of loss of water molecule and denaturation of the protein at 51 °C and 82 °C, which combined into one single lowered peak (250.7 °C) after encapsulation of

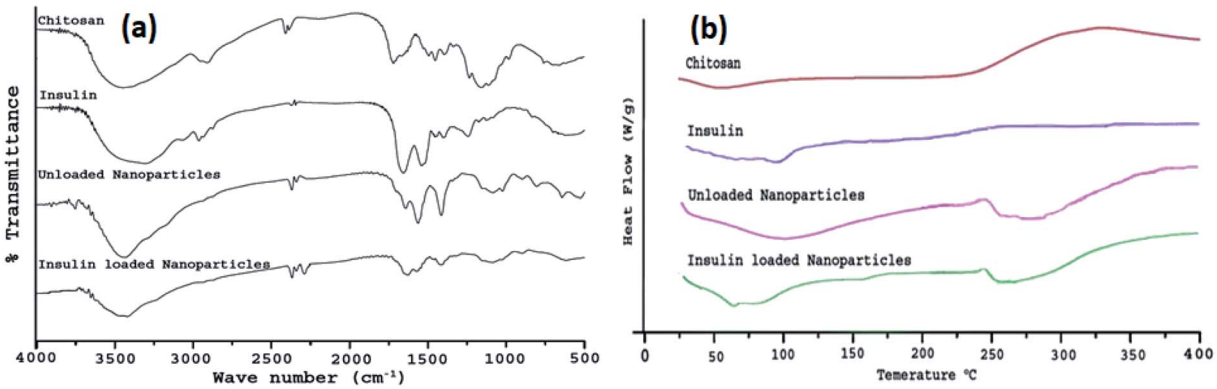

Fig. 3 (a) FTIR spectra of chitosan, insulin, unloaded nanoparticles, and insulin loaded nanoparticles (C4T4I4); (b) DSC thermogram of chitosan, insulin, unloaded nanoparticles, and insulin loaded nanoparticles (C4T4I4).

insulin within chitosan nanoparticles leading to the evidence of insulin in loaded nanoparticles (Fig. 3b).

The denaturation of pure insulin corresponds to the covalent modification of protein or amino acid residues to invent a new molecule *via* cleavage of the bond or new bond formation, rearrangement, or substitution. Unloaded nanoparticles showed varied exothermic thermal peaks at 271.3 °C, 285.7 °C, and 331.4 °C giving an assumption to the formation of stable polyelectrolyte complexes.

3.4. *In vitro* studies

3.4.1. *In vitro* drug release studies. The *in vitro* drug release studies of insulin from chitosan particles revealed a slow release profile compared to free insulin, which released 99% within 4 h. C4T4I4 showed a percent cumulative drug release of 77.23 ± 2.1% after 12 h. Release studies' results suggested that the chitosan nanoparticles can provide a sustained release of insulin for up to 12 h in simulated tear fluid (pH 7.4) due to the better encapsulation in comparison to other optimized formulations. These results lead to an assumption that the *in vitro* release of insulin seems to be continuous to time, and the amount of insulin released gradually increases with time from nanoparticles and the observed release pattern indicates a diffusion-based release mechanism. The *in vitro* drug release kinetics from the nanoparticles was established by determining the diffusion release exponent (η) from the plot of log cumulative drug release *vs.* log time.

The value of diffusion release exponent (η), was 0.71 indicating that the release rate of the drug from the nanoparticles follows a non-Fickian diffusion pattern.[44] Hence, a linear connexion was attained amid a cumulative percent of drug release *versus* time (Fig. 4a).

3.4.2. *Ex vivo* transcorneal permeability studies. The permeation of insulin from optimized nanoparticles through the corneal membrane after 12 h was 73.4 ± 4.8% (Fig. 4b). This result reveals good mucoadhesive and better permeation property of chitosan particles. It was assumed that the chitosan nanoparticles had better retention and more persistent interaction with the ocular surface compared to plain drug solution. The longer contact time and good permeation of chitosan particles yield a high amount of insulin transfer through the cornea. A clear significant difference was observed for samples from 4 h onwards. The reason behind good permeation of chitosan particles can be attributed to the interaction between positively charged chitosan nanoparticles with the intact negatively charged corneal membrane.[45] The insulin loaded permeated particles across the cornea released the insulin in a sustained manner, and thus the drug transport observed here is somewhat similar to the *in vitro* drug release pattern. However, the same is not true with the free insulin as the cornea didn't permit much passage of plain insulin and therefore poor permeation was observed with this sample.

3.5. *In vivo* studies

3.5.1. *In vivo* tolerance studies. From the ocular irritation test of the optimized formulation, after visual examination of the rabbit's eyes, it was found that there was no sign of discomfort in the experimental animal model's eyes. The score of discharge was minimum; the conjunctival hyperemia was low at the 16th hour of experimentation. The corneal opacity score was zero at all observations. The *in vivo* results for the C4T4I4 batch showed a slight sign of irritation at the conjunctiva in one population of the group at the 16th hour, though it only persisted for a very short duration. Hence, it could be addressed that the developed formulation exhibited no toxic or damaging effects to ocular tissues in rabbit eyes which indicates the safety and biocompatibility of the formulation. The observations for conjunctival and eyelid swelling were nil (Table 2).

3.5.2. *In vivo* anti-diabetic studies. *In vivo* anti-diabetic studies were performed on diabetic rabbits. Rabbits were grouped properly and were fasted for the proper assessment of diabetic induction. After streptozotocin administration, animals that showed blood glucose level more than 300 mg dl^{-1} confirmed the induction of diabetes and were taken for further studies. The fluctuation in blood glucose level after ocular administration of plain insulin, as well as insulin loaded nanoparticles, was compared. It was observed that the insulin-loaded nanoparticles led to a significant reduction in elevated glucose levels compared to plain insulin in 6 h *via* the ocular

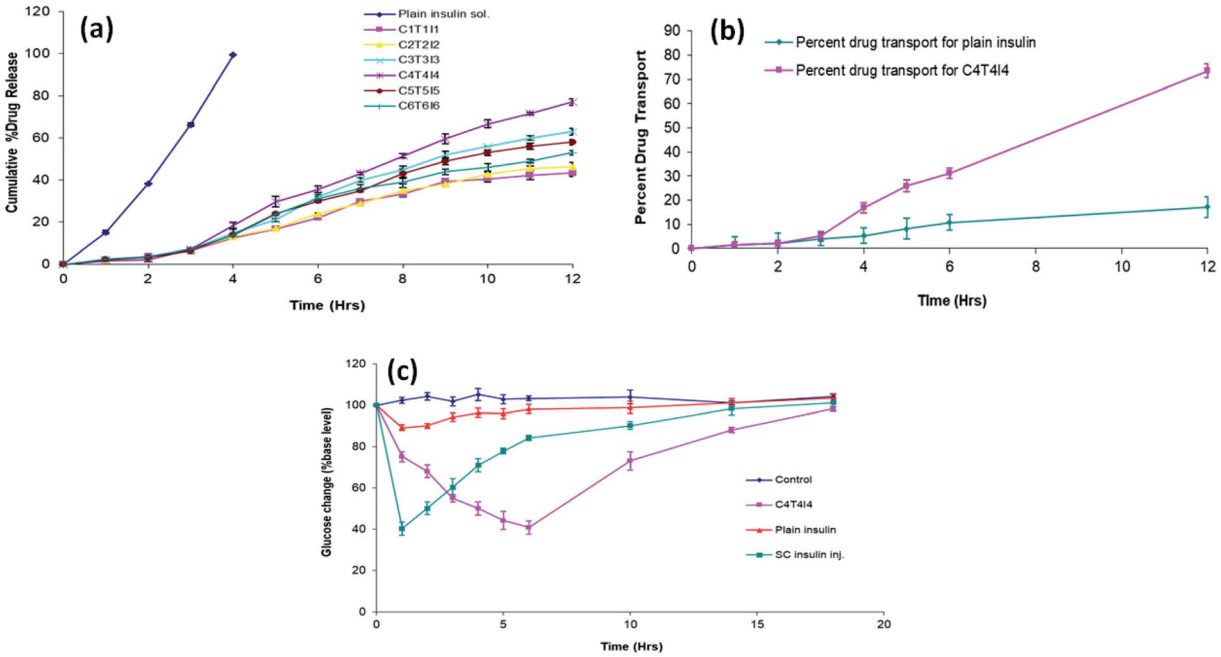

Fig. 4 (a) *In vitro* release profile of developed formulations ($n = 3$); (b) *ex vivo* drug permeation efficiency of plain insulin and C4T4I4 ($n = 3$); (c) blood glucose level (% of increased initial level) in diabetic rabbits after ocular administration of control, optimized C4T4I4, plain insulin solution, and subcutaneous insulin injection ($n = 3$).

route. Fig. 4c exhibited the blood glucose level after the ocular administration of plain insulin and chitosan formulation.

Upon the ocular administration of plain insulin solution, blood glucose level dropped to 89.02 ± 1.41 from the initial blood glucose level after 1 h. This less reduction in blood glucose could be due to the less retention as well as mucosal permeability of the insulin. A drop in blood glucose level was observed by C4T4I4 and SC insulin inj. at 10 h and 4 h which was 73.15 ± 4.38 and 71.08 ± 3.24 respectively. The ocular administration of C4T4I4 showed a delayed but more prominent response in blood glucose reduction when equated with plain insulin *i.e.* 40.69 ± 0.66% of the initial blood glucose level after 6 h. Sample readings were further analyzed by multiple *t*-test and compared with the control group. For the plain insulin sample, the difference in blood glucose level compared to control was found to be non-significant except for the first 2 h. This suggests a short duration of action and poor permeation and adhesion/retention of insulin only sample *via* ocular route. On the contrary, a reduction in blood glucose level observed for the C4T4I4 sample was found to be significant for all tested time points compared to control and plain insulin.

This could be due to the better mucosal permeability of chitosan with increased retention of insulin at the absorption site that leads to effective systemic absorption of insulin *via* the ocular route. The effect was prolonged with C4T4I4 due to the sustained release of insulin from nanoparticles. Subcutaneous insulin injection produced an immediate reduction in blood glucose level, but the effect was not prolonged because of rapid clearance. Though the precision of subcutaneous insulin injection wasn't attained, yet prolonged and controlled insulin release was observed upon the ocular instillation of C4T4I4. Moreover, better acceptance and safety of chitosan

Table 2 Grading system of the macroscopic signs in the *in vivo* tolerance studies of insulin loaded chitosan nanoparticles[a]

Grade	Time								
	Control			Plain insulin solution			C4T4I4		
Time	0.5 h	4.0 h	16.0 h	0.5 h	4.0 h	16.0 h	0.5 h	4.0 h	16.0 h
Discomfort	0	0	0	0	0	0	0	0	0
Discharge	0	0	0	0	1	0	1	0	0
Cornea	0	0	0	0	0	0	0	0	0
Conjunctiva	0	0	0	0	0	0	0	0	1
Lids	0	0	0	0	0	0	0	0	0

[a] $n = 3$.

nanoparticles was established *via* ocular delivery in this study on experimental animal's eyes.

3.5.3. Pharmacokinetic studies. The plot of insulin concentration against time in the rabbit's blood after instillation of 20 μl of subcutaneous insulin injection, optimized nanoparticle formulation (C4T4I4), and plain insulin are exhibited in Fig. 5a. The pharmacokinetic parameters of insulin in plasma were calculated using the trapezoidal rule and the method of residuals. Pharmacokinetic parameters can reflect the dynamic changes of drugs in the body. Thus, from the obtained plasma concentration *vs.* time profile graph, it was found that the plasma concentration of optimized nanoparticles was expressively higher than that of plain insulin solution. Further, the statistical analysis confirmed the significant difference between both samples. The size of the AUC reflects the size of bioavailability. As shown in Table 3, it was evident that the AUC of optimized nanoparticles C4T4I4 significantly increased as compared to that of plain insulin solution ($p \leq 0.05$). The AUC of subcutaneous insulin injection was 197.38 ± 2.76 μg h ml^{-1}. Also, C_{max} of subcutaneous insulin injection was noted at 99.9 with a T_{max} of 0.5 h. C_{max} and T_{max} of optimized nanoparticles were 33.8 ± 3.1 μg ml^{-1} and 4.0 h which was approximately 19-fold that of plain insulin solution (1.8 μg ml^{-1} and 0.33 h) (Fig. 5a).

3.6. Stability studies

Stored C4T4I4 exhibited an increase in the particle size which might have occurred due to the aggregation of the particles

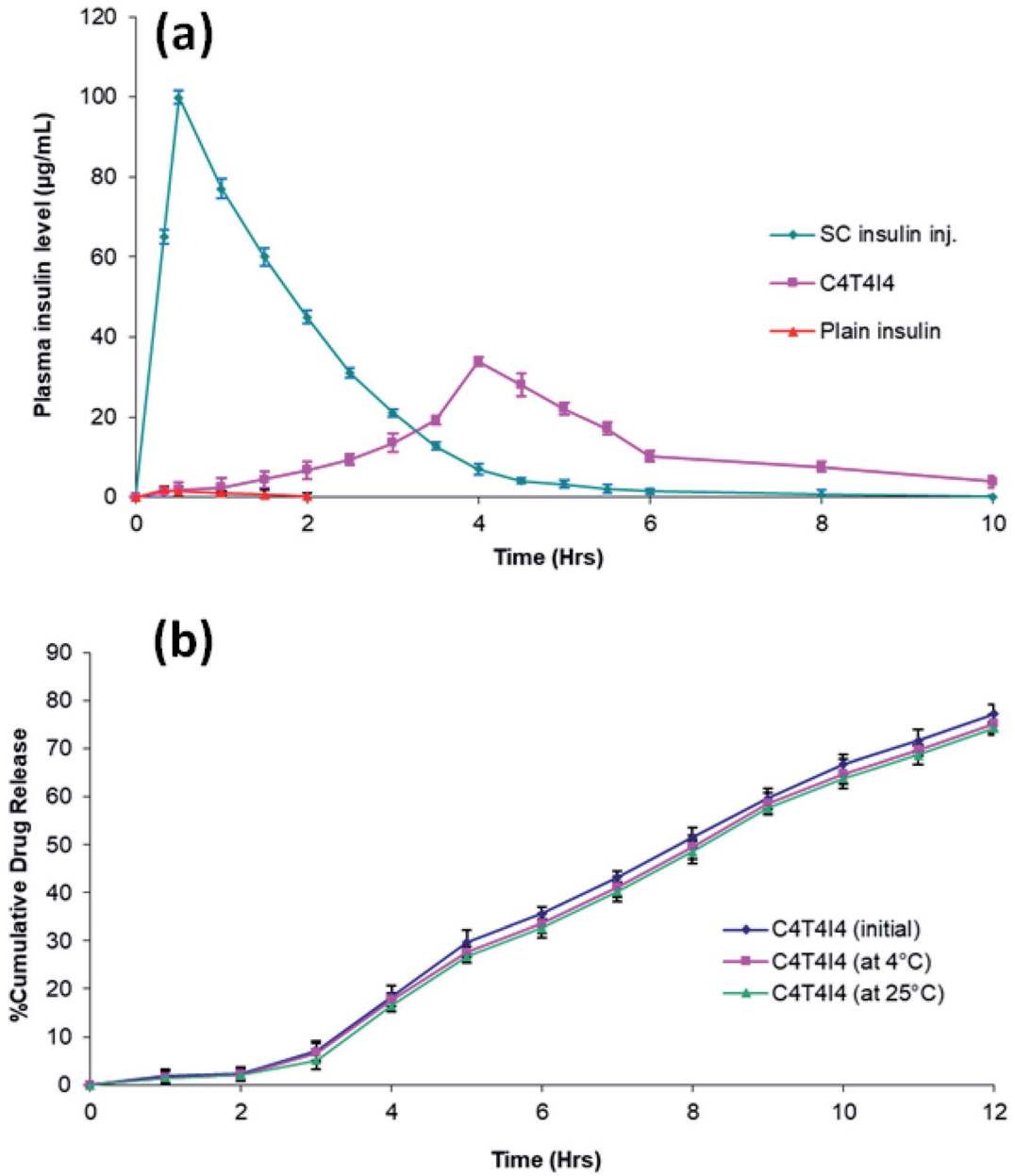

Fig. 5 (a) Pharmacokinetics profile of C4T4I4 compared with plain insulin solution and subcutaneous insulin injection; (b) comparative *in vitro* release profile of C4T4I4 before and after stability studies.

Table 3 *In vivo* ocular absorption study parameters for insulin loaded nanoparticles, plain insulin solution, and subcutaneous insulin injection[a]

Formulation	C_{max}(μg ml^{-1})	T_{max} (h)	AUC_{0-12} (μg h ml^{-1})
C4T4I4	33.8 ± 3.1	4.0	127.16 ± 2.4
Plain insulin solution	1.8 ± 0.28	0.33	1.87 ± 1.7
Subcutaneous insulin injection	99.9 ± 0.32	0.5	197.38 ± 2.76

[a] All values are presented as mean ± SD; $n = 3$.

Table 4 Particle size and Entrapment efficiency studies of optimized C4T4I4 before and after six-month storage[a]

S. no.	Studies	C4T4I4 before storage (initial batch)	C4T4I4 after six-month storage at 4 ± 1 °C (final batch)	C4T4I4 after six-month storage at 25 ± 1 °C (final batch)
1	Average particle size	215 ± 2.5 nm	237 ± 6.67 nm	243 ± 3.31 nm
2	Entrapment efficiency	65.89% ± 4.3	57.22% ± 3.34	51.52% ± 6.24

[a] All values are presented as mean ± SD; $n = 3$.

(Table 4). A lessening in the percent entrapment efficiency was detected from 66% to 52% after the specified stowage period which might be due to the drug seepage (Table 4). The drug release pattern from the stored C4T4I4 displayed similar drug release behavior as that of the freshly prepared C4T4I4 batch (Fig. 5b). Thus, from the obtained results, the insulin loaded chitosan nanoparticles can be considered stable under the tested conditions.[46]

4. Conclusion

Chitosan nanoparticles for ocular administration of insulin were successfully prepared by ionotropic gelation method using tripolyphosphate (TPP) anions, which produced particles of nano-size with positive zeta potential. SEM analysis of particles revealed that particles were spherical with smooth and cross-linked surfaces. It was observed that TPP concentration influenced the particle size and encapsulation efficiency and the optimum ratio found for TPP in this study is (1 : 0.4 : 1, chitosan: TPP: insulin). FTIR and DSC spectra suggested that insulin was efficaciously encapsulated within chitosan particles. The *in vitro* drug release suggested the sustained release of insulin from chitosan particles and followed a non-Fickian diffusion mechanism.

The insulin loaded chitosan particles efficiently permeates through the corneal membrane compared to free insulin as observed in the *ex vivo* drug permeation study. *In vivo* tolerance tests revealed that the formulation is safe and non-toxic to the ocular tissues. Disappearance of the nanoparticles from the eye as well as from the body is another parameter which can be investigated in the coming future. From previous study conducted, the researchers reported the desertion time of the nanoparticles from the vitreous humour was around 24 hours.[47] *In vivo* antidiabetic studies showed prolonged and prominent blood glucose reduction with the aid of chitosan nanoparticulate formulation. Pharmacokinetic studies showed that C4T4I4 could increase insulin systemic absorption through the eyes. The superior activity of insulin loaded chitosan particles compared to free insulin can be attributed to the mucoadhesiveness, enhanced residence time, and improved permeation properties of chitosan. The chitosan nanoparticles had better retention and more persistent interaction with the ocular surface compared to plain drug solution. Besides, insulin loaded chitosan nanoparticles can be considered stable during long-term storage. Hence, it could be concluded from this study that the positively charged chitosan nanoparticles have potentiality in the ocular administration of proteins and peptides like insulin.

Declaration

This research received no external funding.

Compliance with ethical standards

All animal experiments were conducted according to the CPCSEA (Committee for the Purpose of Control and Supervision of Experiments on Animals) guidelines, India (Prevention of Cruelty to Animals Act, 1960) with approval number: EP/PEP/19/C1309 from the Institutional Animal Ethics Committee (IAEC).

Conflicts of interest

The authors declare that they have no conflict of interest.

Acknowledgements

The authors would like to thank AIIMS, New Delhi, India, and Punjab University, Chandigarh, India, for characterization studies.

References

1 R. Shah, M. Patel, D. Maahs and V. Shah, *Int. J. Pharm. Invest.*, 2016, **6**, 1.
2 B. J. Bruno, G. D. Miller and C. S. Lim, *Ther. Delivery*, 2013, **4**, 1443–1467.
3 L. Heinemann, A. Pfutzner and T. Heise, *Curr. Pharm. Des.*, 2005, **7**, 1327–1351.
4 A. Maroni, L. Zema, M. D. Del Curto, A. Foppoli and A. Gazzaniga, *Adv. Drug Delivery Rev.*, 2012, **64**, 540–556.
5 J. S. Patton and P. R. Byron, *Nat. Rev. Drug Discovery*, 2007, **6**, 67–74.
6 V. V. Khutoryanskiy, *Macromol. Biosci.*, 2011, **11**, 748–764.
7 M. R. Prausnitz and R. Langer, *Nat. Biotechnol.*, 2008, **26**, 1261–1268.
8 E. Renard, *J. Diabetes Sci. Technol.*, 2008, **2**, 735–738.
9 G. P. Misra, R. S. J. Singh, T. S. Aleman, S. G. Jacobson, T. W. Gardner and T. L. Lowe, *Biomaterials*, 2009, **30**, 6541–6547.
10 C. Ward, M. Peterson, H. Chandler, A. Hartwick, T. Plageman and A. Sharma, *Insulin Stimulates Protein Synthesis via RTK-Induction of the Akt-s6k Pathway in Human and Canine Corneal Cells*, Ohio, 2019.
11 R. T. Addo, A. Siddig, R. Siwale, N. J. Patel, J. Akande, A. N. Uddin and M. J. D'Souza, *J. Microencapsulation*, 2010, **27**, 95–104.
12 M. A. Woodruff and D. W. Hutmacher, *Prog. Polym. Sci.*, 2010, **35**, 1217–1256.
13 R. C. Nagarwal, S. Kant, P. N. Singh, P. Maiti and J. K. Pandit, *J. Controlled Release*, 2009, **136**, 2–13.
14 M. de la Fuente, M. Raviña, P. Paolicelli, A. Sanchez, B. Seijo and M. J. Alonso, *Adv. Drug Delivery Rev.*, 2010, **62**, 100–117.
15 J. Renukuntla, A. D. Vadlapudi, A. Patel, S. H. S. Boddu and A. K. Mitra, *Int. J. Pharm.*, 2013, **447**, 75–93.
16 S.-J. Cao, S. Xu, H.-M. Wang, Y. Ling, J. Dong, R.-D. Xia and X.-H. Sun, *AAPS PharmSciTech*, 2019, **20**, 190.
17 M. Dash, F. Chiellini, R. M. Ottenbrite and E. Chiellini, *Prog. Polym. Sci.*, 2011, **36**, 981–1014.
18 H. Gupta, T. Velpandian and S. Jain, *J. Drug Targeting*, 2010, **18**, 499–505.
19 S. Mao, U. Bakowsky, A. Jintapattanakit and T. Kissel, *J. Pharm. Sci.*, 2006, **95**, 1035–1048.
20 A. Jintapattanakit, V. B. Junyaprasert, S. Mao, J. Sitterberg, U. Bakowsky and T. Kissel, *Int. J. Pharm.*, 2007, **342**, 240–249.
21 X. Yongmei and D. Yumin, *Int. J. Pharm.*, 2003, **250**, 215–226.
22 B. A. Jitendra, P. K. Sharma and S. Bansal, *Indian J. Pharm. Sci.*, 2011, **73**, 367–375.
23 M. Pandey, H. Choudhury, C. X. Yi, C. W. Mun, G. K. Phing, G. X. Rou, B. J. K. A. A. J. Singh, A. N. A. Jhee, L. K. Chin, P. Kesharwani, B. Gorain and Z. Hussain, *Curr. Drug Targets*, 2018, **19**, 1782–1800.
24 R. Srinivasan and S. K. Jain, *Drug Deliv. J. Deliv. Target. Ther. Agents*, 1998, **5**, 53–55.
25 A. Yamamoto, A. M. Luo, S. Dodda-Kashi and V. H. Lee, *J. Pharmacol. Exp. Ther.*, 1989, **249**, 249–255.
26 P. Calvo, C. Remuñán-López, J. L. Vila-Jato and M. J. Alonso, *J. Appl. Polym. Sci.*, 1997, **63**, 125–132.
27 M. Joseph, H. M. Trinh, K. Cholkar, D. Pal and A. K. Mitra, *Expert Opin. Drug Delivery*, 2017, **14**, 631–645.
28 E. Cevher, Z. Orhan, L. Mulazımoglu, D. Sensoya, M. Alper, A. Yıldıza and Y. Ozsoy, *Int. J. Pharm.*, 2006, **317**, 127–135.
29 A. Anitha, V. G. Deepagan, V. V. Divya Rani, D. Menon, S. V. Nair and R. Jayakumar, *Carbohydr. Polym.*, 2011, **84**, 1158–1164.
30 S. Wadhwa, R. Paliwal, S. R. Paliwal and S. P. Vyas, *J. Drug Targeting*, 2010, **18**, 292–302.
31 A. Mahor, S. K. Prajapati, A. Verma, R. Gupta, A. K. Iyer and P. Kesharwani, *J. Colloid Interface Sci.*, 2016, **483**, 132–138.
32 M. Kaur, A. Bhatia, D. Sethi, G. Kaur and K. Vij, *J. Drug Delivery Ther.*, 2017, **7**, 70–76.
33 M. A. Elgadir, M. S. Uddin, S. Ferdosh, A. Adam, A. J. K. Chowdhury and M. Z. I. Sarker, *J. Food Drug Anal.*, 2015, **23**, 619–629.
34 K. Sonaje, K. J. Lin, S. P. Wey, C. K. Lin, T. H. Yeh, H. N. Nguyen, C. W. Hsu, T. C. Yen, J. H. Juang and H. W. Sung, *Biomaterials*, 2010, **31**, 6849–6858.
35 H. Almeida, M. H. Amaral, P. Lobao, C. Frigerio and J. M. Sousa Lobo, *Curr. Pharm. Des.*, 2015, **21**, 5212–5224.
36 G. Sharma, A. R. Sharma, J.-S. Nam, G. P. C. Doss, S.-S. Lee and C. Chakraborty, *J. Nanobiotechnol.*, 2015, **13**, 74.
37 D. Achouri, K. Alhanout, P. Piccerelle and V. Andrieu, *Drug Dev. Ind. Pharm.*, 2013, **39**, 1599–1617.
38 T. Kissel and V. B. J. A. Jintapattanakit, *Mahidol Univ. J. Pharm. Sci.*, 2008, **35**, 1–7.
39 A. A. Mahmoud, G. S. El-Feky, R. Kamel and G. E. A. Awad, *Int. J. Pharm.*, 2011, **413**, 229–236.
40 C. Gonçalves, P. Pereira and M. Gama, *Materials*, 2010, **3**, 1420–1460.
41 B. Sarmento, D. Ferreira, F. Veiga and A. Ribeiro, *Carbohydr. Polym.*, 2006, **66**, 1–7.
42 B. Sarmento, A. Ribeiro, F. Veiga and D. Ferreira, *Colloids Surf., B*, 2006, **53**, 193–202.
43 J. R. Azevedo, R. H. Sizilio, M. B. Brito, A. M. B. Costa, M. R. Serafini, A. A. S. Araújo, M. R. V. Santos, A. A. M. Lira and R. S. Nunes, *J. Therm. Anal. Calorim.*, 2011, **106**, 685–689.
44 T. H. H. Gatti, J. O. Eloy, L. M. B. Ferreira, I. C. Da Silva, F. R. Pavan, M. P. D. Gremião and M. Chorilli, *Braz. J. Pharm. Sci.*, 2018, **59**, e1734.
45 M. R. Avadi, A. M. M. Sadeghi, N. Mohamadpour Dounighi, R. Dinarvand, F. Atyabi and M. Rafiee-Tehrani, *ISRN Pharm.*, 2011, **2011**, 1–6.
46 H. Katas, M. A. G. Raja and K. L. Lam, *Int. J. Biomater.*, 2013, 1–10, DOI: 10.1155/2013/146320.
47 A. Shafie and M. Fayek, *J. Clin. Exp. Ophthalmol.*, 2013, **4**, 2, DOI: 10.4172/2155-9570.1000273.